Route to high-T_{c} superconductivity via CH_{4}-intercalated H_{3}S hydride perovskites

Wenwen Cui, Tiange Bi, Jingming Shi, Yinwei Li, Hanyu Liu, Eva Zurek, and Russell J. Hemley

Phys. Rev. B **101**, 134504 — Published 9 April 2020

DOI: 10.1103/PhysRevB.101.134504

New route to high-T_c superconductivity via CH_4 intercalated H_3S

Wenwen Cui,[1] Tiange Bi,[2] Jingming Shi,[1] Yinwei Li,[1,*] Hanyu Liu,[3,4,†] Eva Zurek,[2,‡] and Russell J. Hemley[5,§]

[1]*Laboratory of Quantum Materials Design and Application, School of Physics and Electronic Engineering, Jiangsu Normal University, Xuzhou 221116, China*
[2]*Department of Chemistry, State University of New York at Buffalo, Buffalo, NY 14260, USA*
[3]*International Center for Computational Method and Software, College of Physics, Jilin University, Changchun 130012, China*
[4]*International Center of Future Science, Jilin University, Changchun 130012, China*
[5]*Departments of Physics and Chemistry, University of Illinois at Chicago, Chicago IL 60607, USA*

(Dated: February 19, 2020)

While exploring potential superconductors in the C-S-H ternary system using first-principles crystal structure prediction methods, we uncovered a new class of hydrides based on the intercalation of methane into an H_3S framework. These intriguing H_3S-CH_4 structures emerge as metastable at ∼100 GPa. Electron-phonon coupling calculations indicate that phases with the CSH_7 stoichiometry are potential superconductors with T_c values of 100 K and 190 K at 100 GPa and 150 GPa, respectively. The results are expected to guide the experimental search for new high-T_c superconductors, including those stable at lower pressures than previously documented superconducting hydrides such as H_3S and LaH_{10}.

The pursuit of high-T_c and even room-temperature superconductivity has been a grand challenge in physics since the 1911 discovery of superconductivity [1]. Bardeen–Cooper–Schrieffer (BCS) theory [2] can well describe the mechanism for conventional superconductors, opening the door for the discovery and design of high-T_c materials. Ashcroft [3] proposed that compressed hydrides are good candidates for high-T_c superconductors due to chemical 'pre-compression' effects. Subsequent theoretical studies provided explicit predictions of these phenomena, and have led to the discovery of very high temperature superconductivity, first in H_3S (T_c of 203 K) [4] and more recently in LaH_{10} (T_c up to 260 K) [5–7]. These experimental results confirmed theoretical predictions for both the structures and basic mechanism of superconductivity [8–11], thereby marking a new era for both superconductivity and 'materials by design' [5, 12–14]

Compared to binary hydrides, exploration of high-T_c superconductors in ternary hydrides greatly enlarges the configurational space and opens up new chemistry and physics that could in principle enhance both T_c and stability, including at modest pressures. This additional elemental degree of freedom in compressed ternary hydride systems has led to new predicted high-T_c superconductors such as $CaYH_{12}$ (T_c = 258 K at 200 GPa) [15], $LiPH_6$ (T_c = 150-167 K at 200 GPa) [16], and most remarkably Li_2MgH_{16} (T_c = 473 K at 250 GPa) [17]. On the other hand, existing experimental studies have uncovered only relatively low T_c materials such as in $BaReH_9$ (T_c = 7 K) [18] and Li_5MoH_{11} (T_c = 6.5 K) [19]. Returning to sulfur-containing systems, carbon disulfide (CS_2) has been shown to transform to a metal at 50 GPa, and a superconductor with a T_c of ∼6 K at 60-170 GPa [20]. Several ternary hydrides based on the H_3S structure are predicted to exhibit high-T_c behavior, including H_6SSe (i.e., SH_3-SeH_3, with an estimated T_c of 195 K at 200 GPa) [21], Y(La)SH_6 [SH_3-Y(La)H_3, T_c = 95 K and 35 K at 210 GPa and 300 GPa, respectively] [22], and even the noble gas Xe with H_3S (H_3SXe, T_c = 89 K at 240 GPa) [23]. Moreover, several superconductors have also been reported in ternary F-S-H, Y-S-H and B-S-H compounds [24–26].

There is also general interest in carbon-containing high-T_c superconductors. Dense carbides that are isostructural with hydrides have been predicted to exhibit high T_c behavior and to be stable on decompression owing to their rigid carbon sp^3 frameworks [27]. Various hydrocarbons (e.g., CH_4, C_2H_4 and C_2H_6) are stable in different molecular phases to megabar pressures [28–30]. CH_4 and Mg are predicted to form CH_4Mg, a potential superconductor with a T_c of 84-121 K at 75 to 120 GPa [31]. The related compound CH_4K has a predicted T_c of about 12 K at 80 GPa [32]. These results encouraged us to theoretically search for high-T_c superconductors in the C-S-H ternary system. As shown in detail below, metastable Cm and $R3m$ symmetry phases were found, and electron-phonon coupling calculations revealed that both are potential superconductors with T_cs of 97-108 K at 130 GPa and 181-194 K at 150 GPa, respectively as estimated by solving the Eliashberg equations numerically using the typical choice of the Coulomb potential, $\mu^* = 0.10$–0.13.

We began by identifying stable structures in the C-S-H system, focusing on $C_xS_yH_z$ (x = 1-2; y =1-2; z = 1-8) compositions at megabar pressures (100-200 GPa), using heuristic algorithms based on particle swarm optimization [33–35] and evolutionary algorithms [36] in combination with first-principles theory (computational details are provided in the Supporting Information, SI [37]). The CSH_7 stoichiometry emerged as being particularly stable relative to the elements in the pressure range considered. The enthalpies of formation from the elemental phases for CSH_7 were -83, -72, -61, and -25 meV/atom at 100, 130, 150 and 200 GPa, respectively. Interestingly, the structures of CSH_7, shown in Fig. S1 of the SI, are composed of CH_4 molecules intercalated within

* yinwei_li@jsnu.edu.cn
† hanyuliu@jlu.edu.cn
‡ ezurek@buffalo.edu
§ rhemley@uic.edu

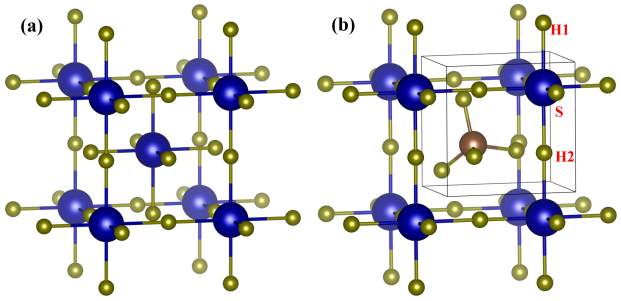

FIG. 1. (a) H_3S ($Im\bar{3}m$ structure), and (b) the $R3m$ symmetry methane intercalated H_3S compound, CSH_7. The brown, blue and yellow-green spheres denote C, S and H atoms, respectively (see the Supplemental Material [37] for more detailed structural information).

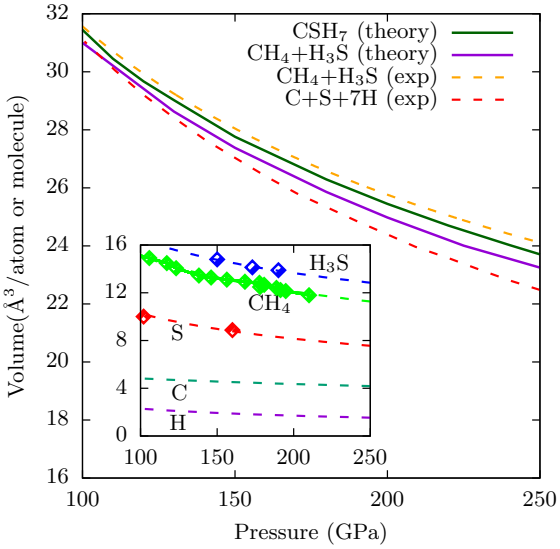

FIG. 2. Calculated CSH_7 EOS compared with the molecular assemblage CH_4+H_3S, and the assemblage C+S+7/2H_2. The green and violet line represent theoretical values: for CSH_7, and the sum of the volume of CH_4 ($Cmca$) [43] + H_3S ($R3m$ and $Im\bar{3}m$) [9]. The insert shows the experimental EOS for H_2 [44], C [45], S [46], CH_4 [47] and H_3S [48]; the points are the measured data.

different, but related, H_3S networks. At 100 GPa, the H_3S sublattice is characterized by SH_5 layers. Upon compression ($\sim$130 GPa), the $R3m$ phase shown in Fig. 1 becomes enthalpically favored, with CH_4 molecules intercalated into the cubic H_3S framework formed by two neighboring SH_5 layers that are linked via shared H atoms.

Although the enthalpies of formation of the CSH_7 phases are negative with respect to the elemental phases, these species do not lie on the 3D convex hull. In fact, they are metastable with respect to CH_4 + H_3S (and CH_4 + H_2S + 1/2H_2), but stable relative to H_2S + C + 5/2H_2 below 188 GPa. The zero-point energy (ZPE) uncorrected enthalpy of $R3m$ is 33 meV/atom above the convex hull at 130 GPa. As shown in Table S1 of the SI, inclusion of the ZPE or finite temperature effects does not stabilize the ternary phase. It should however be noted that a number of compressed hydrides found to be metastable via first-principles calculations have been synthesized in the laboratory. Examples include a Ca_2H_5 phase, which was calculated to be 20 meV/atom above the convex hull [38], and hydrides of phosphorus, which are at least 30 meV/atom above the convex hull [39–41]. Moreover, these phases could potentially be stabilized by anharmonic or nuclear quantum effects as found for LaH_{10} [42]. Therefore, it is expected that the CSH_7 phases could be realized experimentally, especially if they are calculated to be dynamically stable.

The relative enthalpies of the CSH_7 phases between 100 to 300 GPa are shown in Fig. S2. The Cm phase is calculated to transform to $R3m$ at 130 GPa, followed by a transition to $Amm2$ symmetry at 250 GPa. Phonon calculations reveal that Cm is dynamically stable from 100 to 110 GPa, whereas $R3m$ is dynamically stable from 130 to 300 GPa, and $Amm2$ is not dynamically stable at the current level of approximation at 250 and 300 GPa (Fig. S3). Molecular dynamics simulations (Fig. S4), on the other hand, suggest that Cm, $R3m$ and $Amm2$ are stable at 130, 150, and 250 GPa at 300 K, respectively.

The three predicted 0 K structures of CSH_7 and cubic $Im\bar{3}m$ H_3S are shown in Fig. 1 and Fig. S1. In pure H_3S, the S atoms form a bcc lattice with each S atom octahedrally coordinated by H atoms (Fig. 1a). The CSH_7 phases are based on the H_3S structure with the central SH_6 unit replaced by a CH_4 molecule, and a distortion of the cubic framework. In the Cm phase (Fig. S1a), the cubic H_3S lattice is replaced by two layers of SH_5. The H-S distance between neighboring SH_5 layers is too long (1.906 Å) to form an H-S covalent bond. On compression the Cm phase transforms to $R3m$ at 130 GPa (Fig. 1b). In this structure, the H_3S framework is retained but with a slight rhombohedral distortion such that the $\vec{a}$, $\vec{b}$, and $\vec{c}$ unit cell vectors are equal in length, but the α, β, and γ angles measure 89.4° (instead of 90°). The rotation barrier of the CH_4 unit in $R3m$-CSH_7 was estimated to be $<$1 meV/atom at 150 GPa (Fig. S5), suggesting the molecule may rotate freely. At 250 GPa the $Amm2$ phase, with a slightly distorted SH_3 lattice, becomes enthalpically favored (Fig. S1b).

In order to explore the bonding in the CSH_7 phases, their electronic localization functions (ELFs) were plotted (Fig. S6). The ELF is useful for visualizing covalent bonds and lone pairs; it maps values in the range from 0 to 1, where 1 corresponds to perfect localization of the valence electrons indicative of a strong covalent bond. The ELF values for the S-H and C-H bonds are close to 0.9, indicating their strong covalent character. The Cm structure is characterized by 5 S-H bonds (bond lengths of 1.38 to 1.55 Å) and one lone electron pair (Figs. S6a and b). Similar to free methane, the CH_4 units contain 4 strong covalent C-H bonds, as shown in the 3D ELF plots. In the $R3m$ structure, the cubic H_3S framework is clearly evident.

The calculated pressure-volume equation of states (EOS) of

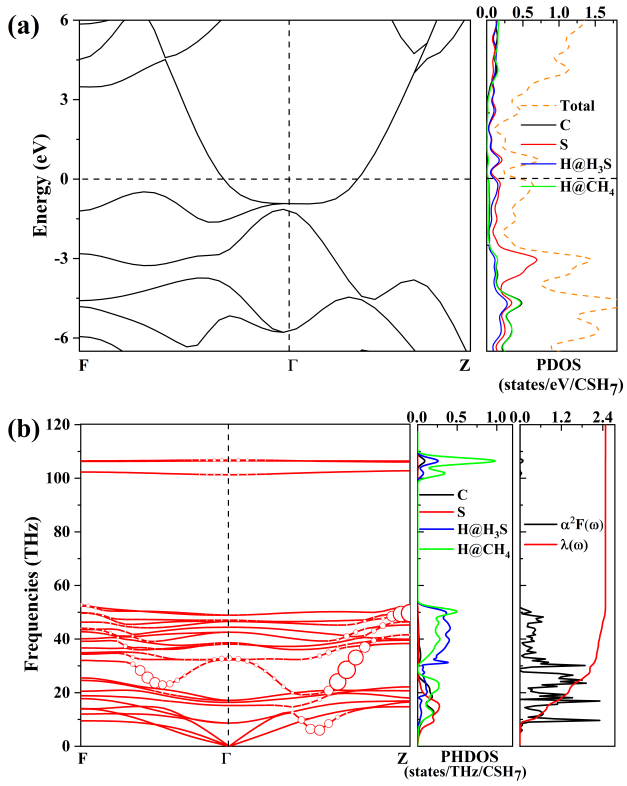

FIG. 3. Calculated (a) band structure, total DOS, and site-projected DOS near the Fermi level, and (b) phonon dispersion curves, PHDOS projected on the C, S and H atoms, Eliashberg spectral function, $\alpha^2F(\omega)$, and $\lambda(\omega) = \int_0^\omega d\omega' 2\alpha^2F(\omega')/(\omega)'$ for CSH_7 ($R3m$ structure) at 150 GPa. Red solid circles represent the phonon line width with the radius proportional to the respective coupling strength.

CSH_7 and assemblages consisting of CH_4 and H_3S, as well as C+S+7/2H_2, are shown in Fig. 2. The sum of the volume of the predicted CH_4 ($Cmca$) [43] and H_3S ($R3m$ and $Im\bar{3}m$) [9] phases is also plotted for comparison. The evolution of the volume under pressure of CSH_7 falls between the experimental and theoretical data obtained for CH_4+H_3S. As shown in Fig. S7, the PV contribution to the enthalpy favors the assemblages over CSH_7 within this pressure range. The pressure dependence of select S-H distances are plotted in Fig. S8. Under pressure the S1-H and S2-H bonds in the Cm phase approach each other, and the S3-H distance decreases, as the phase undergoes pressure induced bond equalization. Because the CH_4 molecule breaks the symmetry, the S-H1 and S-H2 bonds in the $R3m$ phase differ slightly. Both S-H bonds in $R3m$-CSH_7 are slightly shorter than those calculated for $Im\bar{3}m$ H_3S, whose highest T_c, 203 K, was measured at 155 GPa [4]. If the S-H distance, which can be modulated by the identity of the intercalant molecule as well as the pressure, is an important factor in determining the T_c, it is expected that the maximum value for CSH_7 would be at smaller pressures, near the $R3m$ to Cm structural instability.

The band structures and partial densities of states (DOS) for CSH_7 of $R3m$ and Cm were calculated to further explore their electronic properties (Fig. 3a and Fig. S9a). Both exhibit metallic features, wherein the states near the Fermi level are mainly from the contribution of the H_3S framework, with negligible character from the CH_4 molecules. The significant overlap of states with H and S character indicates strong H-S hybridization under pressure, which has been demonstrated to play a key role in driving the high-T_c superconductivity of cubic H_3S [12].

TABLE I. The calculated electron phonon coupling parameter (λ), logarithmic average phonon frequency (ω_{log}), and the estimated T_c of CSH_7 using the Allen-Dynes modified McMillan (ADM) equation [49], and numerically solving the Eliashberg equations [50] with μ^*= 0.10 (0.13).

				T_c (K)	
phase	pressure (GPa)	λ	ω_{log} (K)	ADM	Eliashberg
Cm	100	1.20	1091	98 (86)	108 (97)
$R3m$	150	2.47	925	152 (143)	194 (181)
	200	1.35	1379	137 (128)	158 (144)
	250	0.88	1738	95 (82)	-
	300	0.82	1730	85 (70)	-

Fig. 3b and Fig. S9b show the phonon dispersions, projected phonon density of states (PHDOS), Eliashberg spectral function, $\alpha^2F(\omega)$, and electron-phonon coupling integral, $\lambda(\omega)$, for $R3m$ and Cm CSH_7, respectively. A notable feature of the CH_4 intercalation in the structures is the separation of the vibrational modes into three well distinct regions: the lower frequencies (below 20 THz) are associated with the heavier S, and C atoms, and modes including some of the CH_4 hydrogens; the intermediate frequencies (between 30 and 63 THz) are derived from combinations of H-wagging, bending, and stretching modes; and the higher frequencies ($\sim$100 THz, 3300 cm^{-1}) primarily from the C-H stretching modes of the molecular CH_4 units, close to the asymmetric stretching modes of free CH_4 ($\sim$97 THz, 3200 cm^{-1}).

The superconducting properties of the CSH_7 phases were estimated by the Allen-Dynes modified McMillan equation [49], using typical values of the Coulomb pseudopotential, μ^*= 0.13-0.1. As shown in Table 1, below 250 GPa λ was calculated to be appreciable for both phases. At 100 GPa λ was 1.2 and ω_{log} was 1091 K for the Cm phase, yielding a T_c of 86-98 K. For $R3m$ at 150 GPa, λ was 2.47, which is twice the value found for Cm and comparable to that calculated for cubic H_3S at 200 GPa (λ= 2.19) [9], resulting in a T_c of 143-152 K. The logarithmic average phonon frequency of $R3m$ CSH_7 at 150 GPa is somewhat lower than that of $Im\bar{3}m$ H_3S at 200 GPa [9], 925 K vs. 1335 K, which is the reason for the slightly lower T_c of the ternary. The increase in λ for $R3m$ as compared to Cm is not unreasonable in view of the differences in their phonon band structures. In $R3m$, there are two obvious Kohn anomalies and softened modes at 18-32 THz located along the F-Γ, and Γ-Z high symmetry lines, which contribute a significant amount ($\sim$36%) to λ. In addition, λ of

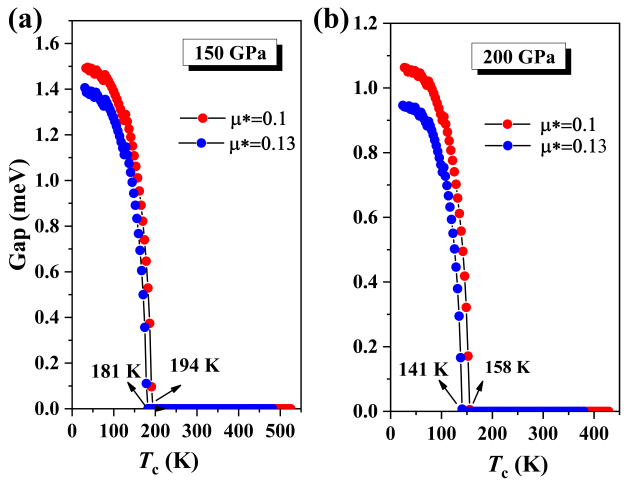

FIG. 4. Calculated anisotropic superconducting gap of CSH_7 ($R3m$ structure) at (a) 150 GPa, and (b) 200 GPa.

$R3m$ was found to decrease with increasing pressure, which was not offset by the increase in $\omega_{\log}$ so that T_c decreased from 150 to 300 GPa. The maximum T_c for CSH_7 therefore occurs at a slightly lower pressure than for H_3S. For strongly coupled superconductors ($\lambda > 1.5$), Eliashberg theory [50] gives a better estimate of T_c, and therefore we also numerically solved the Eliashberg equations for select pressures, as shown in Table I and Fig. 4. As expected, the estimated T_c values were higher, 181–194 K and 141–158 K for $R3m$ at 150 GPa and 200 GPa.

In summary, we have explored the stability and electronic properties of $C_xS_yH_z$ ternary compounds at high pressure. Stoichiometric CSH_7 was found to be dynamically stable above 100 GPa, and two phases with Cm, and $R3m$ space group symmetries were found. Interestingly, these structures are characterized by CH_4 intercalated into a distorted H_3S framework, which could represent a new class of high-temperature superconductors. Electron-phonon coupling calculations indicate that CSH_7 phases are promising conventional superconductors with T_cs estimated to be as high as $\sim$200 K. The results are expected to stimulate the search for other high-T_c H_3S intercalation compounds and more chemically complex hydride superconductors, especially in carbon-bearing systems. Just like pressure, the size of the intercalant molecule can be used to modulate the H-S framework, and thereby to tune its properties, such as T_c. Additional theoretical studies would be useful to examine the effects of quantum and anharmonic dynamics on the calculated critical temperatures and stability of this class of materials, as well as mechanisms for enhancing their phase stabilities at lower pressures.

W.C., J.S. and Y.L. acknowledge funding from the National Natural Science Foundation of China under Grant Nos. 11804128, 11804129 and 11722433. Y.L. acknowledges funding Qing Lan Project of Jiangsu Province. W.C. and J.S. acknowledge the Project Funded by Jiangsu Normal University under Grant No. 18XLRS004 and No. 18XLRS003. R.J.H. acknowledges support from the U.S. National Science Foundation (DMR-1809783). T.B. acknowledges the NSF (DMR-1827815) for financial support. This material is based upon work supported by the U.S. Department of Energy, Office of Science, Fusion Energy Sciences under Award Number DE-SC0020340 to R.J.H. and E.Z. Calculations were performed using the High Performance Computing Center of the School of Physics and Electronic Engineering of Jiangsu Normal University, and the Center for Computational Research at SUNY Buffalo.

W.C. and T.B. contributed equally to this work.

[1] D. Van Delft and P. Kes, Phys. Today **63**, 38 (2010).
[2] J. Bardeen, L. N. Cooper, and J. R. Schrieffer, Phys. Rev. **108**, 1175 (1957).
[3] N. W. Ashcroft, Phys. Rev. Lett. **92**, 187002 (2004).
[4] A. Drozdov, M. Eremets, I. Troyan, V. Ksenofontov, and S. Shylin, Nature **525**, 73 (2015).
[5] R. J. Hemley, M. Ahart, H. Liu, and M. Somayazulu, in *Proc. Ramn Areces Symp. "Superconductivity and Pressure: A Fruitful Relationship on the Road to Room Temperature Superconductivity"*, edited by M. Á. Alario-Franco (Madrid, Spain, May 2122, 2018) pp. 199–213.
[6] M. Somayazulu, M. Ahart, A. K. Mishra, Z. M. Geballe, M. Baldini, Y. Meng, V. V. Struzhkin, and R. J. Hemley, Phys. Rev. Lett. **122**, 027001 (2019).
[7] A. Drozdov, P. Kong, V. Minkov, S. Besedin, M. Kuzovnikov, S. Mozaffari, L. Balicas, F. Balakirev, D. Graf, V. Prakapenka, and et al., Nature **569**, 528 (2019).
[8] Y. Li, J. Hao, H. Liu, Y. Li, and Y. Ma, J. Chem. Phys. **140**, 174712 (2014).
[9] D. Duan, Y. Liu, F. Tian, D. Li, X. Huang, Z. Zhao, H. Yu, B. Liu, W. Tian, and T. Cui, Sci. Rep. **4**, 6968 (2014).
[10] H. Liu, I. I. Naumov, R. Hoffmann, N. Ashcroft, and R. J. Hemley, Proc. Natl. Acad. Sci. U. S. A. **114**, 6990 (2017).
[11] F. Peng, Y. Sun, C. J. Pickard, R. J. Needs, Q. Wu, and Y. Ma, Phys. Rev. Lett. **119**, 107001 (2017).
[12] E. Zurek and T. Bi, J. Chem. Phys. **150**, 050901 (2019).
[13] J. A. Flores-Livas, M. Amsler, C. Heil, A. Sanna, L. Boeri, G. Profeta, C. Wolverton, S. Goedecker, and E. K. U. Gross, Phys. Rev. B **93**, 020508(R) (2016).
[14] P. Cudazzo, G. Profeta, A. Sanna, A. Floris, A. Continenza, S. Massidda, and E. K. U. Gross, Phys. Rev. B **81**, 134506 (2010).
[15] X. Liang, A. Bergara, L. Wang, B. Wen, Z. Zhao, X.-F. Zhou, J. He, G. Gao, and Y. Tian, Phys. Rev. B **99**, 100505(R) (2019).
[16] Z. Shao, D. Duan, Y. Ma, H. Yu, H. Song, H. Xie, D. Li, F. Tian, B. Liu, and T. Cui, npj Comput. Mater. **5**, 1 (2019).
[17] Y. Sun, J. Lv, Y. Xie, H. Liu, and Y. Ma, Phys. Rev. lett. **123**, 097001 (2019).
[18] T. Muramatsu, W. K. Wanene, M. Somayazulu, E. Vinitsky, D. Chandra, T. A. Strobel, V. V. Struzhkin, and R. J. Hemley, J. Phys. Chem. C **119**, 18007 (2015).
[19] D. Meng, M. Sakata, K. Shimizu, Y. Iijima, H. Saitoh, T. Sato, S. Takagi, and S.-i. Orimo, Phys. Rev. B **99**, 024508 (2019).
[20] R. P. Dias, C.-S. Yoo, V. V. Struzhkin, M. Kim, T. Muramatsu, T. Matsuoka, Y. Ohishi, and S. Sinogeikin, Proc. Natl. Acad. Sci. U. S. A. **110**, 11720 (2013).
[21] B. Liu, W. Cui, J. Shi, L. Zhu, J. Chen, S. Lin, R. Su, J. Ma,

K. Yang, M. Xu, J. Hao, A. P. Durajski, J. Qi, Y. Li, and Y. Li, Phys. Rev. B **98**, 174101 (2018).
[22] X. Liang, S. Zhao, C. Shao, A. Bergara, H. Liu, L. Wang, R. Sun, Y. Zhang, Y. Gao, Z. Zhao, and et al., Phys. Rev. B **100**, 184502 (2019).
[23] D. Li, Y. Liu, F.-B. Tian, S.-L. Wei, Z. Liu, D.-F. Duan, B.-B. Liu, and T. Cui, Front. Phys. **13**, 137107 (2018).
[24] S. Zhang, L. Zhu, H. Liu, and G. Yang, Inorg. Chem. **55**, 11434 (2016).
[25] X. Du, S. Zhang, J. Lin, X. Zhang, A. Bergara, and G. Yang, Phys. Rev. B **100**, 134110 (2019).
[26] J. Chen, W. Cui, J. Shi, M. Xu, J. Hao, A. P. Durajski, and Y. Li, ACS omega **4**, 14317 (2019).
[27] S. Lu, H. Liu, I. I. Naumov, S. Meng, Y. Li, J. S. Tse, B. Yang, and R. J. Hemley, Phys. Rev. B **93**, 104509 (2016).
[28] R. J. Hemley and H.-k. Mao, in *AIP Conference Proceedings*, Vol. 706 (AIP, 2004) pp. 17–28.
[29] X.-D. Wen, L. Hand, V. Labet, T. Yang, R. Hoffmann, N. Ashcroft, A. R. Oganov, and A. O. Lyakhov, Proc. Natl. Acad. Sci. U. S. A. **108**, 6833 (2011).
[30] H. Liu, I. I. Naumov, and R. J. Hemley, J. Phys. Chem. Lett. **7**, 4218 (2016).
[31] F. Tian, D. Li, D. Duan, X. Sha, Y. Liu, T. Yang, B. Liu, and T. Cui, Mater. Res. Express **2**, 046001 (2015).
[32] J.-X. Han, H. Zhang, G.-H. Zhong, and et al., Int. J. Mod. Phys. C **30**, 1 (2019).
[33] Y. Wang, J. Lv, L. Zhu, and Y. Ma, Phys. Rev. B **82**, 094116 (2010).
[34] Y. Wang, J. Lv, L. Zhu, and Y. Ma, Comput. Phys. Commun. **183**, 2063 (2012).
[35] B. Gao, P. Gao, S. Lu, J. Lv, Y. Wang, and Y. Ma, Sci. Bull. **64**, 301 (2019).
[36] D. C. Lonie and E. Zurek, Comput. Phys. Commun. **182**, 372 (2011).
[37] See Supplemental Material at [URL will be inserted by publisher], which includes Refs. [51–61]. It contains more detailed computational methods, explicit structural information of the identified stable CSH_7 compounds, the structures of Cm and $Amm2$, as well as additional results on the phase stabilities, zero-point energy effect, the ELF plot, the electron-phonon coupling feature, superconducting properties, etc.
[38] A. K. Mishra, T. Muramatsu, H. Liu, Z. M. Geballe, M. Somayazulu, M. Ahart, M. Baldini, Y. Meng, E. Zurek, and R. J. Hemley, J. Phys. Chem. C **122**, 19370 (2018).
[39] A. Drozdov, M. Eremets, and I. Troyan, arXiv preprint arXiv:1508.06224 (2015).
[40] A. Shamp, T. Terpstra, T. Bi, Z. Falls, P. Avery, and E. Zurek, J. Am. Chem. Soc. **138**, 1884 (2015).
[41] H. Liu, Y. Li, G. Gao, J. S. Tse, and I. I. Naumov, J. Phys. Chem. C **120**, 3458 (2016).
[42] H. Liu, I. I. Naumov, Z. M. Geballe, M. Somayazulu, J. S. Tse, and R. J. Hemley, Phys. Rev. B **98**, 100102(R) (2018).
[43] G. Gao, A. R. Oganov, Y. Ma, H. Wang, P. Li, Y. Li, T. Iitaka, and G. Zou, J. Chem. Phys. **133**, 144508 (2010).
[44] P. Loubeyre, R. LeToullec, D. Hausermann, M. Hanfland, R. Hemley, H. Mao, and L. Finger, Nature **383**, 702 (1996).
[45] A. Dewaele, F. Datchi, P. Loubeyre, and M. Mezouar, Phys. Rev. B **77**, 094106 (2008).
[46] O. Degtyareva, E. Gregoryanz, M. Somayazulu, H.-k. Mao, and R. J. Hemley, Phys. Rev. B **71**, 214104 (2005).
[47] L. Sun, W. Yi, L. Wang, J. Shu, S. Sinogeikin, Y. Meng, G. Shen, L. Bai, Y. Li, J. Liu, and et al., Chem. Phys. Lett. **473**, 72 (2009).
[48] M. Einaga, M. Sakata, T. Ishikawa, K. Shimizu, M. I. Eremets, A. P. Drozdov, I. A. Troyan, N. Hirao, and Y. Ohishi, Nat. Phys. **12**, 835 (2016).
[49] P. B. Allen and R. Dynes, Phys. Rev. B **12**, 905 (1975).
[50] G. Eliashberg, Sov. Phys. JETP **11**, 696 (1960).
[51] G. Henkelman, B. P. Uberuaga, and H. Jónsson, J. Chem. Phys. **113**, 9901 (2000).
[52] D. Sheppard, P. Xiao, W. Chemelewski, D. D. Johnson, and G. Henkelman, J. Chem. Phys. **136**, 074103 (2012).
[53] P. Giannozzi, J. Phys.: Condens. Matter **21**, 395502 (2009).
[54] L. Zhu, H. Liu, C. J. Pickard, G. Zou, and Y. Ma, Nat. Chem. **6**, 644 (2014).
[55] Y. Li, X. Feng, H. Liu, J. Hao, S. A. Redfern, W. Lei, D. Liu, and Y. Ma, Nat. Commun. **9**, 722 (2018).
[56] H. J. Monkhorst and J. D. Pack, Phys. Rev. B **13**, 5188 (1976).
[57] G. Kresse and J. Furthmüller, Phys. Rev. B **54**, 11169 (1996).
[58] G. Kresse and D. Joubert, Phys. Rev. B **59**, 1758 (1999).
[59] J. P. Perdew, K. Burke, and M. Ernzerhof, Phys. Rev. Lett. **77**, 3865 (1996).
[60] J. Shi, W. Cui, S. Botti, and M. A. L. Marques, Phys. Rev. Mater. **2**, 023604 (2018).
[61] Y. Li, J. Hao, H. Liu, S. T. John, Y. Wang, and Y. Ma, Sci. Rep. **5**, 9948 (2015).